Presenilin-1 280Glu→Ala Mutation Alters C-Terminal APP Processing Yielding Longer Aβ Peptides: Implications for Alzheimer's Disease

Gregory D Van Vickle,[1] Chera L Esh,[1] Tyler A Kokjohn,[1,2] R Lyle Patton,[1] Walter M Kalback,[1] Dean C Luehrs,[1] Thomas G Beach,[3] Amanda J Newel,[3] Francisco Lopera,[4] Bernardino Ghetti,[5] Ruben Vidal,[5] Eduardo M Castaño,[6] and Alex E Roher[1]

[1]The Longtine Center for Molecular Biology and Genetics, Sun Health Research Institute, Sun City, Arizona, USA; [2]Department of Microbiology, Midwestern University, Glendale, Arizona, USA; [3]W H Civin Laboratory of Neuropathology, Sun Health Research Institute, Sun City, Arizona, USA; [4]Department of Neuropathology Neuroscience Group, University of Antioquia, Colombia; [5]Indiana Alzheimer Disease Center, Department of Pathology and Laboratory Medicine, Indiana University, Indianapolis, Indiana, USA; [6]Fundacion Instituto Leloir, Buenos Aires, Argentina

Presenilin (PS) mutations enhance the production of the Aβ42 peptide that is derived from the amyloid precursor protein (APP). The pathway(s) by which the Aβ42 species is preferentially produced has not been elucidated, nor is the mechanism by which PS mutations produce early-onset dementia established. Using a combination of histological, immunohistochemical, biochemical, and mass spectrometric methods, we examined the structural and morphological nature of the amyloid species produced in a patient expressing the PS1 280Glu→Ala familial Alzheimer's disease mutation. Abundant diffuse plaques were observed that exhibited a staining pattern and morphology distinct from previously described PS cases, as well as discreet amyloid plaques within the white matter. In addition to finding increased amounts of CT99 and Aβ42 peptides, our investigation revealed the presence of a complex array of Aβ peptides substantially longer than 42/43 amino acid residue species. The increased hydrophobic nature of longer Aβ species retained within the membrane walls could impact the structure and function of plasma membrane and organelles. These C-terminally longer peptides may, through steric effects, dampen the rate of turnover by critical amyloid degrading enzymes such as neprilysin and insulin degrading enzyme. A complete understanding of the deleterious side effects of membrane bound Aβ as a consequence of γ-secretase alterations is needed to understand Alzheimer's disease pathophysiology and will aid in the design of therapeutic interventions.

Online address: http://www.molmed.org
doi: 10.2119/2007-00094.Van Vickle

INTRODUCTION

Alzheimer's disease (AD) increasingly affects the elderly population and now represents the third most common cause of death among aged adults. As the average life expectancy increases, the number of subjects with AD will rise almost exponentially, with cases estimated to quadruple by the year 2050 (1). The pathologic hallmark of AD is the abundant accumulation of soluble and fibrillar amyloid-β (Aβ) peptides in the extracellular space and vascular walls of the brain. The 40/42(43) amino acid Aβ peptides deposited in AD brains are produced by the sequential proteolytic action of the β- and γ-secretases on a larger, membrane anchored, type-1 β-amyloid precursor protein (βAPP). Shorter Aβ peptides (P3), corresponding to the Aβ sequence residues 17–42, are generated when βAPP is cleaved by the combined sequential activity of α- and γ-secretases. All Aβ peptides have limited water solubility because they contain the hydrophobic βAPP transmembrane domain amino acid sequence.

A second AD characteristic is the intracellular production of neurofibrillary tangles (NFT), mainly composed of hyperphosphorylated tau proteins and remnants of membrane glycolipids (2–4). Associated with the amyloid and NFT accumulation are chronic neuroinflammation and severe vascular alterations. These compromise brain tissue perfusion and aerobic metabolism, resulting in a dramatic loss of synapses, neuronal demise, and gliosis that result in drastic gray and white matter atrophy.

Address correspondence to and reprint requests to *Alex E. Roher, Sun Health Research Institute, 10515 W Santa Fe Drive, Sun City, AZ 85351. Phone: 623-876-5465; Fax: 623-876-5698; E-mail: alex.roher@sunhealth.org.*
Submitted October 1, 2007; Accepted for publication January 14, 2008; Epub (www.molmed.org) ahead of print January 16, 2008.

The presenilins are components of the γ-secretase, a membrane bound aspartyl protease composed of four interacting molecules: presenilin (PS), which contains the protease active center; nicastrin; APH-1; and PEN-2 (5–7). In humans, two PS genes code for the PS1 and PS2 molecules, which are 65% amino acid sequence identical (8).

To date, more than 160 mutations in PS1, 11 in PS2, and 27 in βAPP have been reported (http://www.molgen.ua.ac.be/ADMutations) on the whole, expressing with some degree of variation, an AD phenotype. Many PS mutations increase the production of the β-secretase C-terminal (CT) 99 amino acid-long fragment (CT99), which is subsequently cleaved by the γ-secretase to yield the Aβ peptides (CL Esh and AE Roher, unpublished observations). There is evidence that during this process the γ-secretase first cleaves at the ε-site of βAPP (corresponding to the Aβ sequence of residues 49–50) to produce a transcription factor known as the βAPP intracellular domain (AICD). The γ-secretase or an uncharacterized carboxypeptidase(s) then hydrolyzes at the γ-site to generate the Aβ42 peptide (9,10), although some evidence supports the tenet that the production of Aβ and AICD are two entirely γ-secretase independent phenomena (11).

It is widely accepted that the PS mutations cause neurodegeneration and dementia by influencing βAPP processing to yield Aβ42 preferentially (12). Moreover, the early age of onset in familial Alzheimer's disease (FAD) due to PS mutations appears to correlate with an increase in Aβ42 and a corresponding decrease in Aβ40 levels (13). Another characteristic shared by some PS mutations is the generation of large quantities of Aβ peptides N-terminally truncated at residue 3, and more abundantly at residue 11 (14,15), suggesting that PS mutations influence both β- and γ-secretase activities. However, in transgenic mice, some PS mutations cause neurodegeneration in the absence of Aβ peptides, indicating that Aβ generation, per se, may not be necessary for all aspects of AD development (16).

We investigated the chemical composition of the Aβ-related peptides derived from a demented patient carrying the PS1 280Glu→Ala mutation. This autosomal dominant mutation is particularly prevalent in the area of Medellin, Colombia.

Besides the anticipated increased amount of CT99, Aβ42 and abundant diffuse plaques, our investigation revealed the presence of peptides substantially longer than 42/43 amino acid residue species. These longer Aβ peptides may have significant implications for understanding the pathogenesis and development of both FAD and sporadic AD (SAD).

MATERIALS AND METHODS

Clinical Report (PS1 280Glu→Ala)

A 49-year-old male patient manifested progressive loss of short-term memory and declining manual abilities over a 3-year period. In addition, the patient also reported depression, irritability, loss of verbal fluency, changes in personality, and hyperphagia, but still was capable of managing activities of daily living. An EEG revealed no abnormal wave patterns and thyroid function was within normal range. The family history revealed the patient's mother suffered from dementia at age 43. Two years later, the hyperphagia continued, memory loss was estimated at about 80%, and partial deficits in the ability to perform daily living activities and aimless wandering were evident. The patient was delusional, suffered severe insomnia, nominal aphasia, and exaggerated reflex responses. At age 52, the patient began to hallucinate, had advanced aphasia, occasional myoclonus, aggravated insomnia, and Parkinsonian gait. At this stage, the hyperphagia disappeared. The patient was incapable of managing the activities of daily living, was incontinent and exhibited severe weight loss. At age 54, the patient was totally aphasic and amnesic. He also exhibited Parkinsonian symptoms of sialorrhea, dysphagia, rigidity, and myoclonus as well as experiencing two to three seizures a day. The patient died at 54 years of age.

Neuropathology

Autopsy performed in the immediate postmortem (3.3 h postmortem interval) revealed severe cerebral atrophy (brain weight 1053 g), more apparent in the frontal, parietal, and temporal lobes. Paraffin sections (6 μm) were obtained from the frontal, parietal, and temporal areas and stained with hematoxylin and eosin (H&E), Campbell-Switzer silver technique, and thioflavine-S. Immunocytochemistry was carried out using the polyclonal antibody against Aβ40 (anti-Aβ 5074P; Chemicon/Millipore, Billerica, MA, USA) at 1:300 dilution. Aβ42 was detected using the 21F12 monoclonal antibody (Elan, South San Francisco, CA, USA) at 1:1000 dilution. Polyclonal anti-Aβ AβN3pE (IBL, Gunma, Japan) was used to detect pyroglutamyl modifications at Aβ residue 3 (1:100 dilution). The monoclonal antibody (AT8 Polymedco, Cortland Manor, NY, USA) was employed at 1:300 dilution to detect tau phosphorylation at Ser202 and Thr205 residues.

Quantitation of Aβ Peptides by Immunoassay

One hundred mg of frontal cerebral cortex from the PS1 280Glu→Ala and two non-demented (ND) control cases were homogenized in 800 mL of 5 M guanidine-HCl, 50 mM Tris-HCl pH 8.0 with an electric grinder at 4°C. After 3 h of continuous shaking, the specimens were centrifuged at 60,000*g* in a Ti 50.4 Beckman rotor for 30 min at 4°C. The supernatants were collected and submitted to ELISA analysis using the anti-Aβ40 and anti-Aβ42 antibodies (Immuno-Biological Laboratories, Minneapolis, MN, USA and Immunogenetics, Belgium) according to the manufacturers' instructions.

Separation of Peptides by Size-Exclusion Chromatography

Three grams of cerebral cortex from a subject expressing the PS1 280Glu→Ala

mutation were dissected from the subjacent white matter and homogenized with 20 mL of 90% glass distilled formic acid (GDFA) in a Potter-Elvehjem glass tissue grinder. After standing at room temperature (RT) for 15 min, the homogenate was decanted into two polyallomer tubes and centrifuged for 1 h at 40,000*g* (SW 41Ti rotor Beckman rotor) at 5°C. The lipid layers floating at the top of the tubes were discarded and the GDFA clear supernatant (18 mL) collected. Half of the GDFA-soluble sample (9 mL) was aliquoted into 500 µL microfuge tubes that were individually submitted to fast protein liquid chromatography (FPLC), on a size-exclusion Superose 12 column (1 cm × 30 cm; Amersham/General Electric, Piscataway, NJ, USA) equilibrated and developed with 80% (v/v) GDFA at a flow rate of 15 mL/h at RT. Eluate absorbance was monitored at 280 nm. The fractions corresponding to a M_r of 10–2 kDa were collected and pooled, 5 mL of a 10% (w/v) solution of the zwitterion betaine was added, and the fraction volumes were reduced to 200 µL by vacuum centrifugation (Savant/GMI, Ramsey, MN, USA). To minimize contamination from proteins in regions flanking the collected fractions, the collected 10–2 kDa fractions were pooled and subjected to a second round of FPLC purification under the same conditions to generate six final 10–2 kDa samples which were volume-reduced, labeled as GDFA-soluble fraction, and stored at –80°C.

Separation of Peptides by Reverse-Phase Chromatography

The GDFA-soluble fraction FPLC specimens containing the 10–2 kDa peptides were fractionated further using high performance liquid chromatography (HPLC) with a reverse-phase Zorbax 300SB-C8 column (9.4 mm × 250 mm; Agilent, Santa Clara, CA, USA) at 80°C. To enhance the solubility of the Aβ peptides prior to loading, the FPLC 10–2 kDa fractions were reduced by vacuum centrifugation to an approximate volume of 200 µL and 80% GDFA added to produce a final volume of 500 µL for column loading. The chromatography was developed with a mobile phase mixture of solvent 'A': water/0.1% (v/v) trifluoroacetic acid (TFA), and solvent 'B': acetonitrile/0.1% (v/v) TFA, operated at a flow rate of 1.5 mL/min to generate a linear gradient from 20% to 60% acetonitrile in 90 min. Eluate absorbance was monitored at 214 nm. Collected fraction volumes were reduced to 100 mL by vacuum centrifugation and submitted to Western blot, MALDI-TOF and SELDI-TOF mass spectrometry analyses.

One-Dimensional Western Blots

Brain tissue (100 mg) from sporadic AD (SAD), ND age-matched control, and PS1 280Glu→Ala cases were homogenized in 800 mL of 1 X PBS, pH 7.4, containing complete Protease Inhibitor Cocktail (Roche Diagnostics, Mannheim, Germany) at 4°C. Total protein was quantified with the BCA protein assay kit (Pierce). For a complete protocol of SDS-PAGE and Western blotting, see reference 17. The Notch intracellular domain (NICD) was detected with anti-Notch 1 antibody (Chemicon, Temecula, CA, USA). This antibody identifies only the γ-secretase-cleaved form of the Notch protein. Antibody-reactive bands were detected with goat anti-rabbit horseradish peroxidase (HRP)-conjugated secondary antibody from Pierce (Rockford, IL, USA).

Two-Dimensional Western Blots

Fifty mg of gray matter each from the PS1 280Glu→Ala and from two SAD cases (79 and 89 y old), as well as a control case (82 y old), were individually homogenized in 700 mL of homogenization buffer (7 M urea, 2 M thiourea, 4% 3-[3-(cholamidopropyl)dimethylammonio]-1-propanesulfonate hydrate [CHAPS], 1% dithiothreitol [DTT], 40 mM Tris-HCl pH 8, protease inhibitor cocktail [Roche Diagnostics, Mannheim, Germany]). After 20 strokes with a Teflon homogenizer, the samples were sonicated, incubated for 1 h at RT, and then sonicated again. The samples then were centrifuged in a 120.2 TLA rotor (Beckman, Fullerton, CA) at 10,000 g for 20 min at 4°C. The supernatant from each sample was collected and dialyzed against distilled water in 1000 Dalton molecular weight cut-off (MWCO) bags for 3 h (18). The dialyzed samples were sonicated, and a BCA protein assay performed to quantify total protein levels (Pierce). Two hundred µg of total protein was incubated for 30 min at RT in rehydration buffer (9 M urea, 2% [v/v] CHAPS, 2 M thiourea, 1.25% [v/v] IPG buffer pH 3-10 [GE Healthcare, Piscataway, NJ, USA], 18 mM DTT, 0.002% [v/v] bromophenol blue). Rehydrated proteins were equilibrated into 11 cm IPG strips, pH 3–10 (GE Healthcare) for 16 h at RT. First-dimension isoelectric focusing was performed with an Ettan IPGphor system (GE Healthcare) as follows: 1 h at 50 V, 1 h at 100 V, 1 h at 200 V, 1 hr at 400 V, 1 h at 800 V, 1 h at 1600 V, and 1.5 h at 6000 V, to complete a total application of 12,150 V-h. The strips were incubated for 15 min in 5 mL of equilibration buffer containing 50 mM Tris-HCl, 6 M urea, 30% (v/v) glycerol, 2% (v/v) SDS, 0.002% (v/v) bromophenol blue, and 65 mM DTT for 15 min at RT, followed by equilibration in the same buffer with 200 mM iodoacetamide replacing DTT for 15 min at RT. The strips were subjected to second-dimension electrophoresis in Criterion Tris-HCl, 4-20% acrylamide gels (Bio-Rad, Hercules, CA, USA) in 1X Tris/glycine/SDS buffer (Bio-Rad) for 60 min at 200 V. Kaleidoscope prestained protein molecular weight standards (Bio-Rad) were loaded onto each gel. After electrophoresis, the gels were equilibrated for 15 min in 1X Tris/glycine transfer buffer containing 20% (v/v) methanol, and the separated proteins transferred electrophoretically onto 0.45 µm nitrocellulose membranes (Bio-Rad) at 30 V for 1 h. Western blot analysis (17) was performed with an antibody raised against the 9 C-terminal amino acids of βAPP termed CT9APP (Chemicon).

Matrix-Assisted Laser Desorption/Ionization-Time of Flight (MALDI-TOF) Mass Spectrometry (MS)

The HPLC fractions were reduced to ~30 mL and 5 mL samples were added to

5 mL of a saturated solution of α-cyano-4-hydroxycinnamic acid (CHCA), dissolved in 50% (v/v) acetonitrile/0.1% (v/v) TFA. Aliquots of 0.5 mL were spotted on a sample plate, and mass spectra obtained by averaging 100 laser shots on a MALDI-TOF Voyager DE STR mass spectrometer (Applied Biosystems, Foster City, CA, USA). Calibration was made using the CalMix 2 mixture (Applied Biosystems). The characteristics of the MALDI-TOF and the composition of the employed calibration markers are presented elsewhere (17).

Surface Enhanced Laser Desorption Ionization-Time of Flight (SELDI-TOF) Mass Spectrometry (MS)

Selected HPLC peaks in which Western blot analysis revealed the presence of Aβ peptides were dialyzed in 1000 MW cutoff bags for 1 h against 50 mM Tris-HCl, pH 8.0, and 1 h against 10 mM Tris-HCl, pH 8.0. Dialyzed sample volumes were reduced to approximately 50 μl prior to application on ProteinChip arrays. Before sample application, the dialyzed peak samples were sonicated three times for 1 s each. The samples were then analyzed using SELDI-TOF mass spectrometry (Ciphergen/Bio-Rad, Hercules, CA, USA). The PS20 ProteinChip® Arrays were prepared by loading 4 μl PBS onto the chip spots and incubating for 15 min at RT. A volume of 4 μl of the polyclonal anti-Aβ40, and anti-Aβ42 antibodies (Invitrogen, Carlsbad, CA, USA), was loaded onto the chip at 0.38 mg/mL and 0.57 mg/mL, respectively. The antibody-amended protein chips were incubated in a humidity chamber for 1 h at RT. The chip surfaces were blocked with 4μl of ethanolamine (1 M, pH 8.0) for 30 min. The sample spots were individually washed once with 4 μl PBS + 0.5% (vol/vol) Triton X-100 and twice with 4 μl PBS. The protein chips were loaded with either 4 μl of sonicated sample, 4 μl of Aβ 1-40, or 1-42, peptide standards in DMSO (California Peptide Research, Napa, CA, USA) as positive control, and incubated overnight in a humidity chamber at 4°C. After the sample binding solutions were removed, the spots were washed individually—twice with 4 μl PBS + 0.5% Triton X-100, once with 4 μl PBS, and once with 4 μl distilled water. The chips were allowed to air dry and a 20% saturated solution of CHCA in acetonitrile with 0.1% TFA was applied twice (0.5 μl); the chips were allowed to dry between applications. The molecular mass assignments were made by 100 averaged shots in a Ciphergen Seldi Protein Biology System II, with external calibration attained using the Ciphergen All-In-One Peptide Standard.

RESULTS

Microscopic examination of PS1 280Glu→Ala mutation-expressing cerebral cortex tissue showed abundant diffuse plaques which were strongly stained by the Campbell-Switzer silver stain (Figure 1A). These diffuse plaques did not exhibit the morphological and histochemical/immunocytochemical characteristics of the cotton wool plaques (CWP) described in other PS mutations that stained positive for H&E (15,19,20). The diffuse plaques in the PS1 280Glu→Ala mutation were negative for H&E and heterogeneous in size, ranging from 10–110 μm, with irregular shapes and borders, and made of the agglutination of amorphous fluffy material (Figure 1B). Some of these plaques revealed a clearer center, and at times demonstrated the presence of a dense central core with dystrophic neurites. In some instances, several plaques coalesced into larger fused structures. A limited number of plaques fluoresced intensely with thioflavine-S (Figure 1C). Interspersed within the cortex among the diffuse plaques were a moderate number (~5%) of compact amyloid core plaques with brush-like borders, and plaques with loosely aggregated skeins of amyloid fibrils, which were stained intensely by thioflavine-S. Both of these amyloid plaques resembled those observed in SAD patients. Intriguingly, ectopic amyloid plaque cores with brush-like borders were evident in the deep white matter, at times isolated, and in some occasions in clusters (Figures 1D and 1E). A moderate number of blood vessels contained abundant thioflavine-S stain-reactive amyloid in their walls suggesting fibrillar Aβ was present (Figure 1F). The antibody against Aβ N-terminal region, with pyroglutamyl at position 3, demonstrated the presence of AβN3pE in blood vessels with amyloid deposits and compact amyloid core plaques, as well as in a limited number of diffuse plaques (data not shown). In addition, a significant number of neuropil threads, NFT, and diffuse plaques were stained with the anti-tau (AT8) antibody (Figure 1G). All diffuse and core plaques were intensely positive for the anti Aβ42 (21F12) antibody (Figure 1H). By contrast, a very limited number of plaques were positive for the anti-Aβ40 antibody staining (Figure 1I). In agreement with previous characterizations of the PS1 280Glu→Ala mutation, the immunoassays demonstrated that the amount of Aβ42 in the brain was increased (3.27 μg/g wet weight) relative to that of Aβ40 (1.11 μg/g). For comparison, the average amounts of Aβ from 2 ND controls were: 0.12 μg/g wet weight and 0.055 μg/g for Aβ40 and Aβ42, respectively.

To determine whether or not the PS1 280Glu→Ala mutation affected the processing of the APP CT region, 2D Western blots were generated, reacted with anti-CT9APP antibody, and the molecular patterns compared with those obtained from AD and ND cases. The PS1 mutation case evidenced a larger amount of the CT APP peptides (CT99) relative to the amounts seen in one of the AD cases and the ND case (Figures 2A, 2C, 2D). However, after normalizing by density, one of the AD cases showed a slightly higher amount of CT APP peptides (Figure 2B). Western blots of the PS1 280Glu→Ala mutation-expressing cortex reacted with an antibody, raised against the Notch intracellular domain (NICD), showed prominent bands with a Mr of ~50 kDa and ~30 kDa, which were comparatively much fainter in the SAD and ND cases (Figure 2E).

Solubilization of the cerebral cortex by GDFA, followed by centrifugation, effi-

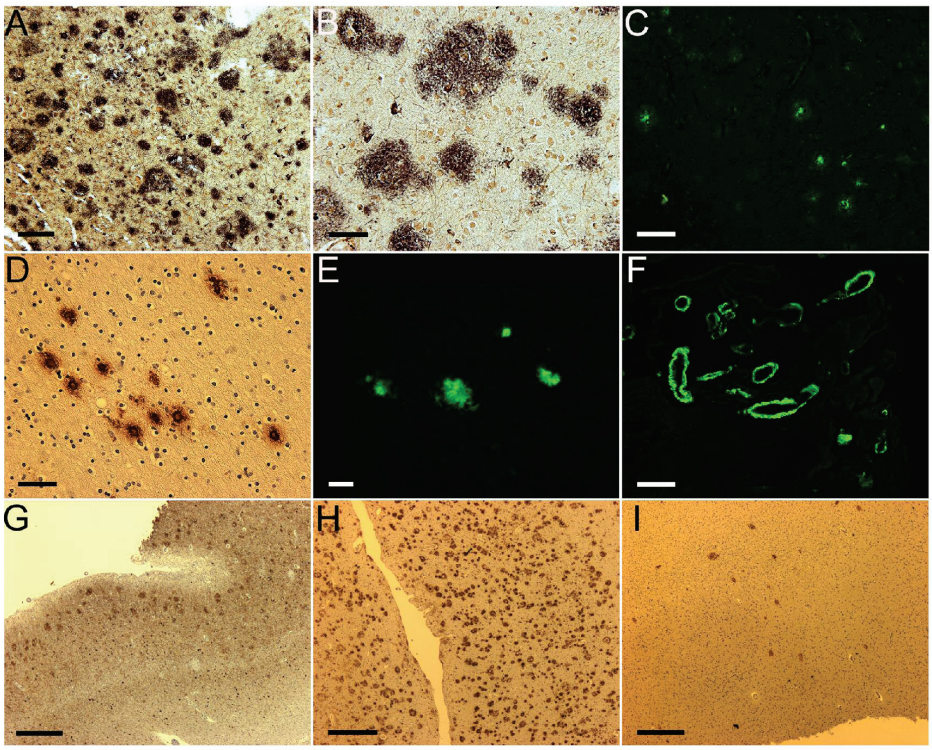

Figure 1. Histochemical and immunohistochemical analyses of PS1 280Glu→Ala cortical and white matter Aβ plaques and tau deposition. A) A field demonstrating the abundant number of plaques at 100 X magnification stained by Campbell-Switzer silver technique. B) At higher magnification (200 X), the plaques appear to be composed of aggregated amorphous fluffy material. C) A reduced number of silver stain-positive plaques also stained by thioflavine-S suggesting the presence of fibrillar amyloid, 100 X magnification. D) A deep white matter cluster of amyloid core plaques stained by 21F12, an Aβ42 antibody. 200 X magnification. E) A group of white matter amyloid core plaques stained by thioflavine-S. Notice the brush-like borders and radiated orientation of the fibrils which resemble the SAD plaque architecture, 200 X magnification. F) A cluster of cortical blood vessels showing fibrillar Aβ deposition. Overall, the cerebro-vascular amyloidosis in the PS 280Glu→Ala is mild to moderate. Thioflavine-S stain, 100 X magnification. G) A large number of diffuse plaques were stained for the AT8 antibody detecting the presence of NFT embedded in these lesions. At higher magnification, the AT8 antibody appears to be concentrated within dystrophic neurites similar to the case for SAD senile plaques. The section also revealed an abundant number of NFT within cortical neurons, 25 X magnification. H) Virtually all diffuse and amyloid plaque in the cerebral cortex stained by the 21F12 antibody raised against Aβ ending at residue 42, 25 X magnification. By contrast, a reduced number of cortical plaques were stained with the Aβ40 antibody, 25 X magnification (I). Scale bars: A, C, F = 100 μm; B, D = 50 μm; E = 20 μm; G, H, I = 500 μm.

ciently separated the lipid membrane fraction that floated as a compact layer at the top of the tube. The supernatant was collected carefully, avoiding contamination with the top lipid and a small pellet containing acid-insoluble proteins, mainly blood vessel cross-linked collagenous material. Separation of the molecules present in the acid supernatant by size-exclusion chromatography yielded two major fractions: larger and smaller than 10 kDa (Figure 3A).

The GDFA-soluble 10-2 kDa fraction obtained from the size-exclusion chromatography was further fractionated by C8 reverse-phase chromatography, which yielded 13 peaks that were investigated by Aβ-Western blotting. Seven fractions harbored Aβ40 and Aβ42 (Figure 3B), with an apparent enrichment of Aβ42 over Aβ40. Interestingly, Western blotting analysis also revealed an unexpected diversity of amyloid peptides with significant amounts of oligomers as well as shorter forms (less than 4,500 M_r).

Mass spectrometry (MS) analyses by MALDI-TOF and SELDI-TOF of the GDFA-soluble fractions, separated by reverse-phase chromatography, confirmed the presence of an array of peptide species corresponding to truncated, complete, and longer Aβ peptide sequences. MALDI-TOF revealed peptides with N-termini from position 1 through 47 and C-termini from position 11 through 55. SELDI-TOF, using the Aβ42 as capture antibody, demonstrated the presence of peptides starting at position 1 through 31 and C-termini from position 37 through 55. Both unmodified and chemically modified Aβ sequences were also represented. Some of the Aβ peptides were modified by oxidation of AβMet35 to Met sulfone or sulfoxide, which increased the Mr in each case by 16 or 32 Daltons. Cyclization of residues Glu3 and/or Glu11 to their pyroglutamyl derivatives were also observed in both the MALDI-TOF and SELDI-TOF mass spectra which, in either case, decreased the Mr by 18 Daltons. Experimentally induced formylation(s) at positions Aβ, Ser8 and Ser26, and Thr43 and Thr48, increased the M_r by 28 Daltons or integral multiples. Table 1 depicts the MALDI-TOF Mr of Aβ peptides with N-termini at residues 1 through 27, and C-termini from residues 44 through 55. The margin of error in all MALDI-TOF spectra between the expected and observed Aβ peptide masses was ± 1 Dalton. SELDI-TOF spectrometry using the Aβ42 capture antibody also demonstrated the presence of Aβ peptides longer than 43 amino acid residues possessing C-termini, ranging from residue 44 through residue 55, as shown in Table 2. The precision for the SELDI-TOF mass determinations was ± 0.1 % Daltons, with an average devia-

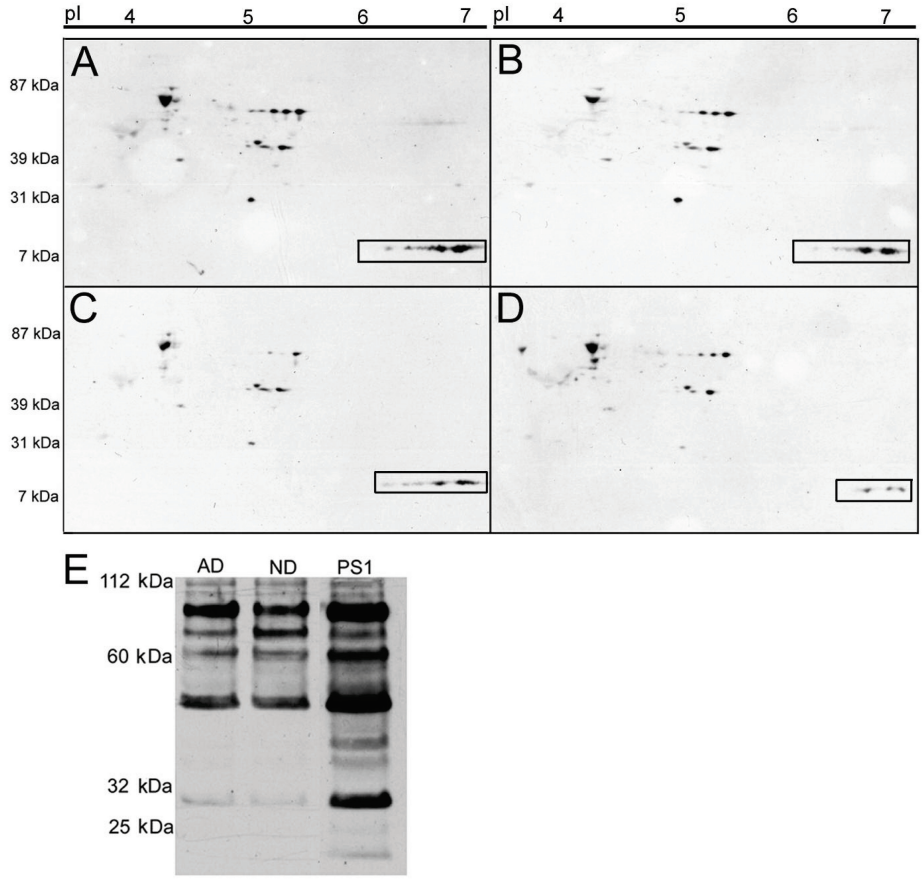

Figure 2. Western blots of PS1 280Glu→Ala mutation, SAD, and ND control samples developed with the anti-CT9APP antibody and with an antibody recognizing the NICD domain. To minimize technical errors, the 2D Western blots (A to D) were executed under the same conditions at the same time using 200 μg of total protein for the PS1, SAD, and ND cases. The CT99 peptide and its post-translationally modified forms are boxed at the bottom right corner of the blots. Scanning densitometry showed that CT99 peptides are more abundant in the PS1 mutation (A) than in one SAD case (C), and the ND control (D). The other SAD case (B) had slightly increased amounts of CT99 peptides after normalizing by density. E) One dimensional Western blot of Notch. The NICD antibody detected prominent bands at ~80, 60, 50 and 30 kDa, which were more pronounced in the PS1 mutation—suggesting a more significant representation of NICD and its degradation by-products. The total protein loaded for SAD, ND, and PS1 was 25 μg.

tion of ± 1.9 Daltons. In addition, the SELDI-TOF spectra suggested three Aβ peptides that extended beyond residue 55 and putatively corresponded to the APP sequences: 29–90, 28–89, and 34–93 (Aβ notation).

DISCUSSION

The PS1 280Glu→Ala mutation yields abundant diffuse plaques with a lesser number of the thioflavine-S-positive amyloid plaques characteristic of SAD, suggesting two fundamentally different neuropathologic mechanisms underlie FAD and SAD. The diffuse amyloid present in this PS1 FAD case was positive for tau, suggesting the presence of dystrophic neurites with autophagic bodies and NFT, and structurally distinct from the PS CWP and SAD diffuse plaques. Another feature of the PS1 280Glu→Ala mutation is the presence of distinct amyloid core plaques within the deep white matter. White matter ectopic neurons have been reported in other PS1 mutations (21,22) that strongly implicate Aβ in PS pathology at this locus. In most PS mutations so far studied, there is a preponderance of peptides ending at residue Aβ42 over those with C-termini at residue Aβ40 (15,23,24). In the present study, the ratio of Aβ40:Aβ42 was 1:3 as determined by ELISA on freshly prepared gray matter homogenates.

γ-secretase expresses a relaxed substrate specificity and has a sufficiently broad substrate specificity to hydrolyze βAPP at multiple sites within the transmembrane domain (25). In addition to βAPP, γ-secretase has the ability to cleave more than 25 different substrates, including Notch, and is capable of establishing stable interactions with more than 40 non-substrate proteins (reviewed in reference 26). This protein complex participates in protein trafficking, calcium metabolism, cell adhesion, synaptic activity, and cell signaling (26), as well as in neurogenesis, neuronal differentiation, neuronal trafficking, and neuronal apoptosis (27–29). In SAD, Notch-1 expression is increased in the hippocampus, suggesting PS mutations may contribute directly to Aβ-induced neuronal death (30,31). However, competition between Notch-1 and βAPP for γ-secretase diminishes net PS1 production of amyloid peptides (32,33). Western blot comparison of Notch-1 proteolysis by-products generated in the cerebral cortices of SAD, ND, and the FAD PS1 280Glu→Ala case showed an increased level of a peptide corresponding to the 80 kDa NICD in the FAD tissue with comparatively lower amounts observed in SAD and ND brains. In the same blot, two additional bands (~50 and 30 kDa) were identified which were reduced greatly in SAD and ND subjects. Therefore, mutations in the PS molecules profoundly affect Notch metabolism and function. Important alterations also occur in the proteolytic degradation of βAPP in the FAD PS1 280Glu→Ala, in which there is an apparent increase in the amount of the CT99 fragment relative to an AD and

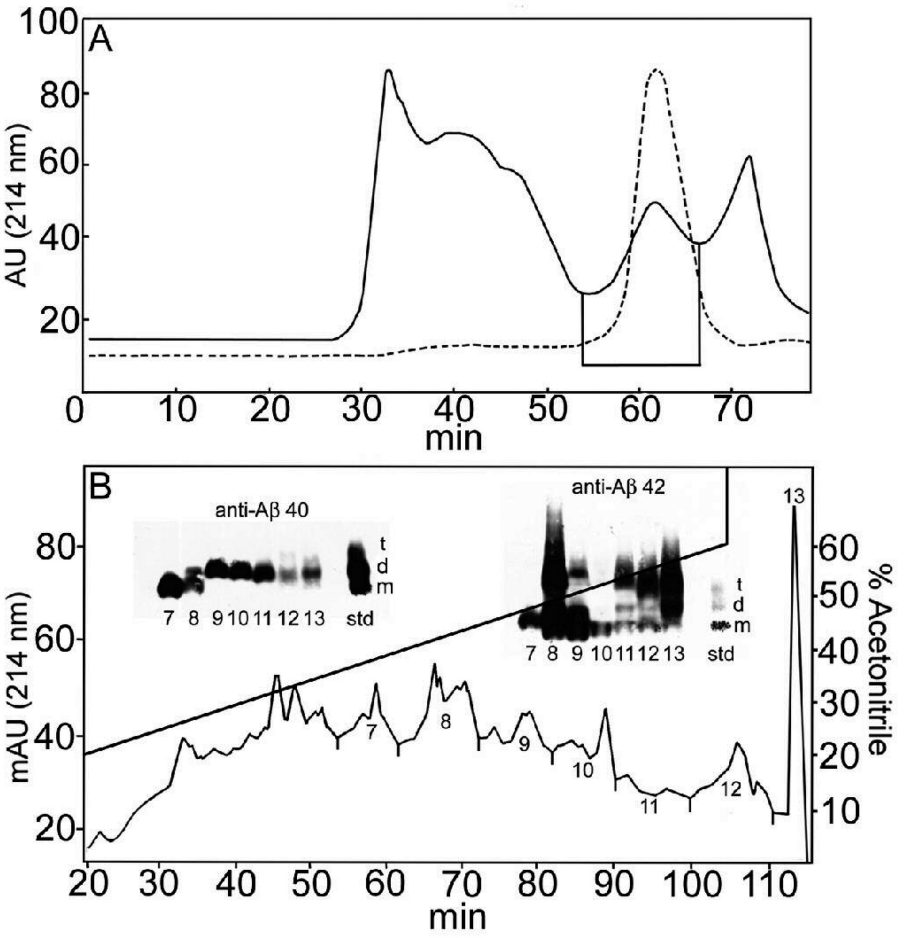

Figure 3. Chromatographic profiles of PS1 280Glu→Ala samples. A) FPLC trace of the acid soluble fraction carried out in a size-exclusion Superose 12 column. The 10–2 kDa fractions, eluted between 54 and 66 min retention (solid line trace) time were pooled from three consecutive runs and re-chromatographed under the same conditions to minimize flanking contaminations (see hyphened trace). B) HPLC chromatographic profile of the 2–10 kDa FPLC fraction separated on a C8 reverse-phase column. All fractions were assessed by Western blots using the Aβ40 and Aβ42 antibodies. The slanted line indicates the slope of the acetonitrile gradient. The abbreviated terms t, d, and m refer to trimer, dimer, and monomer forms, respectively, of Aβ-40 and Aβ-42 standards.

ND control. The more abundant CT99 suggests that a deranged PS1 enzymatic activity due to the mutation leads to the accumulation of this fragment. The CT APP fragment is correlated with neurotoxicity, alterations in calcium metabolism, long-term potentiation, memory failure, free radical generation, and increased production of inflammatory cytokines and chemokines and glyosis (reviewed in reference 34). The consequences of increased levels of CT99 also have been studied in the CT Tg mice overexpressing the carboxy-terminal 100 amino acids of APP. These mice showed profound degeneration of neurons, axons, dendrites, synapses, and cerebral blood vessels (35). Furthermore, intraventricular injection of CT100 in mice induced behavioral impairment (36).

Cerebral cortex homogenization in 80% GDFA solubilizes all the Aβ peptides because it totally disintegrates all cellular and extracellular structures. The acidic supernatant contains the APP/Aβ and proteolytic derivatives, including the hydrophobic transmembrane domain. In the intact brain, these peptides are partitioned among various tissue compartments, such as the cellular membranes and cytosol of neurons, glia, and vascular cells. In addition, the acid fraction also contains the soluble oligomers and insoluble fibrils deposited as extracellular amyloid in plaques and blood vessel walls. The acid extract also includes the Aβ peptides which were in the process of proteolytic degradation.

Previous studies on the Aβ peptides present in cortical amyloid plaque cores and cerebral blood vessels of SAD demonstrated that most of the molecules had C-termini at Val40 and Ala42, with a small fraction terminating at residue Thr43. A significant degree of N-terminal degradation and other post-translational modifications were evident (37–39). The chemical composition of the Aβ peptides was also confirmed in PS2/APP Tg mice amyloid plaques isolated by laser microdissection (LMD) and direct examination by mass spectrometry (40). Characterization of the Aβ peptides in SAD diffuse plaques indicated a mixture of Aβ17-42 (P3) and of Aβ1-42 species (41). Water soluble dimeric/oligomeric Aβ also ends at residues 40/42 (42,43). The amyloid plaques in APP23 and tg2576 transgenic mice carrying the Swedish double mutations also produced Aβ peptides ending at residues 40/42 and possessed characteristics similar to the peptides found in SAD patients (44,45). However, characterization of FAD due to the APP717 Val→Phe Indiana mutation revealed longer Aβ peptides with C-termini at residues Aβ43 through 54 (46) suggesting that γ-secretase cleavage of APP and specificity are substantially perturbed. Likewise, the PDAPP Tg mice carrying the FAD APP 717Val→Phe mutation generated Aβ peptides ending at positions Aβ44 through 62 (17). Additional studies using tgCRND8 Tg mice that carry the Swedish mutations, plus the Indiana mutation, confirmed these results. These mice also demonstrated a

Table 1. MALDI-TOF of PS1 Peptides with C-termini ≥ Aβ 44

Observed Mass	Calculated Mass	Peptide Fragment	Observed Mass	Calculated Mass	Peptide Fragment
4827.81	4828.48	1–45	3071.75	3072.62	14–43
5254.11	5255.04	1–49	4311.65	4311.31	14–54
5483.84	5483.44	2–52	2834.03	2834.37	15–42
5611.79	5611.62	2–53	3573.99	3574.33	15–49
4529.62	4529.16	3–44	3546.03	3545.33	16–50
5069.41	5068.87	3–49	2778.66	2778.31	17–44
4400.46	4400.04	4–44	2891.31	2891.47	17–45
4514.10	4513.20	4–45	3318.02	3318.02	17–49
4612.14	4612.33	4–46	3318.54	3318.02	17–49
4826.66	4826.60	4–48	3417.79	3417.16	17–50
5282.30	5283.25	4–52	3661.98	3661.51	17–52
4892.23	4891.71	5–50	2778.66	2778.31	18–45
5135.68	5136.07	5–52	3091.11	3090.70	18–48
5492.48	5520.60	5–55	2778.66	2778.31	19–46
4096.03	4096.68	6–44	2891.31	2891.47	19–47
4309.90	4308.97	6–46	3335.17	3336.06	19–51
4979.59	4979.89	6–52	3301.20	3302.05	20–52
5108.06	5108.06	6–53	3430.59	3430.22	20–53
4597.66	4598.39	7–50	3557.86	3558.39	20–54
4729.18	4729.58	7–51	3686.10	3686.57	20–55
5226.44	5227.27	7–55	2313.35	2313.74	22–45
4615.14	4614.50	8–51	2071.10	2071.47	23–44
5025.40	5025.10	9–55	2284.09	2283.76	23–46
3601.87	3601.19	10–43	2841.59	2841.51	23–51
3700.33	3700.32	10–44	2069.31	2069.54	24–45
4024.35	4024.77	10–47	2069.31	2069.54	25–46
4469.74	4470.37	10–51	2284.09	2283.80	25–48
4583.60	4583.53	10–52	2867.80	2868.63	25–53
4076.96	4076.86	11–49	2140.40	2139.67	27–48
4420.44	4420.35	11–52	2351.92	2351.96	27–50

novel γ-secretase processing pattern that yielded CT APP fragments ending at residues 44–99, 45–99, 52–99, 54–99 (Aβ sequence numbering). Furthermore, this mouse strain produced a variety of Aβ peptides with C-termini ranging from residues 43 through 55 (47).

Longer Aβ peptides also have been identified in lysates of cells transfected with CT APP and PS1 and PS2 genes, as well as their wild types (PS1wt, PS1 146Met→Leu, PS1 233Met→Thr, PS1 384Gly→Ala, PS2wt, and PS2 141Asn→Ile) when treated with the γ-secretase inhibitor DAPT. These peptides yielded Aβ sequences ending at residues 43, 44, 45, 46, 48, and 49 (48). Human skeletal muscle also produces longer Aβ peptides with C-termini at residues 44, 45, and 46 (49). Recently, CWP were isolated by LMD from FAD patients carrying the PS1 261Val→Ile and PS1 261Val→Phe mutations. Mass spectrometry indicated that the CWP plaques were composed of amino-terminally truncated Aβ peptides, in which the most abundant forms were Aβ 3-42/43 and Aβ11-42/43, with N-terminal pyroglutamyl (15).

The cellular compartments in which the larger and correspondingly more hydrophobic Aβ peptides reside as a consequence of PS1 mutations remain to be established. From a thermodynamic point of view, the cellular plasma and organelle membranes are the candidates of choice. It has been established that the sites of Aβ synthesis are the endoplasmic reticulum, Golgi and plasma membranes where the APP and secretases are located, concentrated within membranes (50,51). In the lipid rafts of neuronal cell lines, APP, β-secretase aspartyl protease (BACE-1), and the four components of the γ-secretase were found (52,53). In the tg2576 Tg mice, lipid rafts apparently contain APP and its CT-fragments, dimeric Aβ peptides, Apo E, tau, PS1, BACE-1, and neprilysin (NEP) (54). The experimental evidence suggests that mutations in the PS and APP genes, such as PS1 280Glu→Ala and APP 717Val→Phe, alter enzyme-substrate specificities and promote the generation of longer, more hydrophobic Aβ peptides that may be retained in membranes. Other PS-like aspartyl proteases may cleave APP to yield a constellation of more massive Aβ peptides such as those generated in FAD patients and FAD-expressing transgenic animals (55). Marchesi (56) recently proposed that in AD, a significant amount of dimeric Aβ peptides could be retained in membranes by the side-to-side interaction of the transmembrane Gly-X-X-X-Gly motifs present in the Aβ sequence (Aβ29–37: Gly-Ala-Ile-Ile-Gly-Leu-Met-Val-Gly-Gly). Curran and Engelman (57) suggested that these intramembranous sequence motifs facilitate dimerization by promoting helix-helix stable interactions as it occurs in soluble coiled-coil structures. The presence of AβThr43 and Thr48 further stabilizes inter-helical hydrogen bonding. The retention of longer length Aβ peptides might be fostered by a proportionally greater representation of hydrophobic transmembrane domains and by changes in the fundamental lipid composition of membranes brought about by the aging process (58,59). In AD, there is a profuse neuritic accumulation of autophagic vacuoles and autophagosomes, represented by dense and multilamellar bodies whose origin still remains unexplained, but may in part result from the retention of longer Aβ peptides and/or of longer membrane-bound Aβ peptides. The presence of APP, CT fragments, and secretases in AD autophagic vacuoles lends support to this contention (60). Au-

Table 2. SELDI-TOF of PS1 Peptides Captured with Aβ42 Antibody with C-termini ≥ Aβ44

Observed Mass	Calculated Mass	Peptide Fragment	Observed Mass	Calculated Mass	Peptide Fragment
4824.83	4828.48	1–45	4417.25	4419.41	12–53
5141.54	5141.88	1–48	3422.06	3422.05	13–45
5357.32	5354.17	1–50	3518.90	3521.19	13–46
5140.05	5139.95	2–49	3382.60	3384.05	14–46
5372.96	5370.28	2–51	4055.06	4054.96	14–52
4532.38	4529.16	3–44	4311.99	4311.31	14–54
4640.23	4642.32	3–45	3358.27	3360.06	15–47
5067.06	5068.87	3–49	3575.36	3574.33	15–49
5169.06	5168.01	3–50	3321.00	3318.02	17–49
4401.68	4400.04	4–44	3661.75	3661.51	17–52
4516.26	4513.20	4–45	3438.07	3435.19	18–51
4824.83	4826.60	4–48	3337.20	3336.06	19–51
5169.06	5170.09	4–51	3575.52	3577.40	19–53
4890.62	4891.71	5–50	3559.66	3558.39	20–54
5139.79	5136.07	5–52	2595.61	2596.11	21–47
5389.45	5392.42	5–54	2595.38	2597.11	21–47
4311.99	4308.97	6–46	2627.90	2627.14	22–48
4640.23	4636.39	6–49	3340.05	3339.14	22–54
5109.74	5108.06	6–53	3339.28	3340.14	22–54
5226.90	5227.27	7–55	2285.36	2283.76	23–46
4055.06	4056.74	8–46	3340.05	3338.20	23–55
4985.72	4984.00	8–54	3339.28	3339.20	23–55
5110.08	5112.18	8–55	2595.38	2595.23	24–50
4640.23	4640.58	9–52	2285.36	2283.80	25–48
4898.58	4896.93	9–54	2627.90	2627.29	25–51
3337.20	3336.90	11–42	2571.46	2570.24	26–51
3646.91	3650.30	11–45	2681.91	2683.40	26–52
4417.25	4420.35	11–52	2353.09	2351.96	27–50
3518.90	3521.19	12–45	2595.38	2596.32	27–52

tophagic programmed cell death may result from endoplasmic reticulum stress caused by unfolded, misfolded, or alternatively folded proteins and their toxic accumulation (reviewed in 61). This type of 'apoptosis' may be triggered by ischemic and hypoxic injuries associated with cerebrovascular disease (61). Strong arguments have recently arisen stating that autophagic activity in dying cells might indeed be a survival strategy (62).

The existence of larger and more hydrophobic Aβ peptides, as the result of γ-secretase dysfunction in FAD PS1 280Glu→Ala, may have a profound impact on their turnover by brain proteases. Among these, NEP and insulin degrading enzyme (IDE), whose genetic deletion leads to Aβ accumulation in mice, show a typical size restriction for peptide substrates (63–65). In the case of NEP, a transmembrane and raft-associated metalloendopeptidase, physiological substrates are limited to 3–4 kDa, due to access limitations to the active site (66). Insulin degrading enzyme, in turn, presents a cavity which is just large enough to enclose an insulin monomer. This enzyme is capable of degrading amyloidogenic peptides associated with neurodegeneration, including Aβ, ABri, and ADan almost exclusively in their unordered monomeric state (67–69). Therefore, longer Aβ peptides generated by mutant PS1 are likely to escape proteolytic clearance—either due to their monomeric size or, more likely, to their high tendency to rapidly dimerize. In addition, increasingly longer hydrophobic C-termini may be selectively retained within the lipid bilayer, thereby imposing a strong thermodynamic restriction to proteolysis.

The relentless net accumulation of Aβ peptides and their longer relatives would greatly disturb membrane function, and result in severe and irreversible neuronal injury. If this hypothesis is proven correct, a new dimension will be added to the understanding of the pathophysiology of AD, and to the design of earlier and novel therapeutic interventions.

ACKNOWLEDGEMENTS

We are in debt to Daniel Brune and John Lopez for technical advice. We are also in great debt to David Rumsey for developing the Amino Acid Mass Search (AAMS) program. This study was supported by the National Institute on Aging (NIA) grants: RO1 AG-19795, the NIA Arizona Alzheimer's Disease Core Center P30 AG19610, the NIA Indiana Alzheimer's disease Center P30 AG10133, The State of Arizona Alzheimer's Research Consortium, the Alzheimer's Association, and COLCIENCIAS project 1115-343-19127, and CODI, 2007-2008 Sustainability Program to the Neuroscience Group, University of Antioquia, Medellín, Colombia.

REFERENCES

1. Brookmeyer R, Gray S, and Kawas C. (1998) Projections of Alzheimer's disease in the United States and the public health impact of delaying disease onset, *Am. J. Public Health*. 88:1337–42.
2. Gray EG, Paula-Barbosa M, and Roher A. (1987) Alzheimer's disease: paired helical filaments and cytomembranes, *Neuropathol. Appl. Neurobiol*. 13:91–110.
3. Goux WJ, Rodriguez S, and Sparkman DR. (1996) Characterization of the glycolipid associated with Alzheimer paired helical filaments. *J. Neurochem*. 67:723–33.
4. Goux WJ, Liu B, Shumburo AM, Parikh S, and Sparkman DR. (2001) A quantitative assessment of glycolipid and protein associated with paired helical filament preparations from Alzheimer's diseased brain. *J. Alzheimers Dis*. 3:455–66.
5. Kimberly WT, LaVoie MJ, Ostaszewski BL, Ye W, Wolfe MS, and Selkoe DJ. (2003) Gamma-secretase is a membrane protein complex comprised of presenilin, nicastrin, Aph-1, and Pen-2. *Proc. Natl. Acad. Sci. U. S. A*. 100:6382–7.
6. Wolfe MS. (2006) The gamma-secretase complex: membrane-embedded proteolytic ensemble. *Biochemistry*. 45:7931–9.

7. Hebert SS et al. (2004) Coordinated and widespread expression of gamma-secretase in vivo: evidence for size and molecular heterogeneity. *Neurobiol. Dis.* 17:260–72.
8. Kopan R and Goate A. (2000) A common enzyme connects notch signaling and Alzheimer's disease, *Genes Dev.* 14:2799–806.
9. Sato T et al. (2003) Potential link between amyloid beta-protein 42 and C-terminal fragment gamma 49-99 of beta-amyloid precursor protein. *J. Biol. Chem.* 278:24294–301.
10. De Strooper B. (2007) Loss-of-function presenilin mutations in Alzheimer disease. Talking Point on the role of presenilin mutations in Alzheimer disease, *EMBO Rep.* 8:141–6.
11. Hecimovic S, Wang J, Dolios G, Martinez M, Wang R, and Goate AM. (2004) Mutations in APP have independent effects on Abeta and CT-Fgamma generation. *Neurobiol. Dis.* 17:205–18.
12. Davis JA et al. (1998) An Alzheimer's disease-linked PS1 variant rescues the developmental abnormalities of PS1-deficient embryos. *Neuron.* 20:603–9.
13. Kumar-Singh S et al. (2006) Mean age-of-onset of familial Alzheimer disease caused by presenilin mutations correlates with both increased Abeta42 and decreased Abeta40. *Hum. Mutat.* 27:686–95.
14. Russo C et al. (2000) Presenilin-1 mutations in Alzheimer's disease. *Nature.* 405:531–2.
15. Miravalle L, Calero M, Takao M, Roher AE, Ghetti B, and Vidal R. (2005) Amino-terminally truncated Abeta peptide species are the main component of cotton wool plaques. *Biochemistry.* 44:10810–21.
16. Saura CA et al. (2005) Conditional inactivation of presenilin 1 prevents amyloid accumulation and temporarily rescues contextual and spatial working memory impairments in amyloid precursor protein transgenic mice. *J. Neurosci.* 25:6755–64.
17. Esh C et al. (2005) Altered APP processing in PDAPP (Val717→Phe) transgenic mice yields extended-length Abeta peptides. *Biochemistry.* 44:13807–19.
18. Van den Bergh G, Clerens S, Cnops L, Vandesande F, and Arckens L. (2003) Fluorescent two-dimensional difference gel electrophoresis and mass spectrometry identify age-related protein expression differences for the primary visual cortex of kitten and adult cat. *J. Neurochem.* 85:193–205.
19. Crook R et al. (1998) A variant of Alzheimer's disease with spastic paraparesis and unusual plaques due to deletion of exon 9 of presenilin 1. *Nat. Med.* 4:452–5.
20. Takao M et al. (2002) A novel mutation (G217D) in the Presenilin 1 gene (PSEN1) in a Japanese family: presenile dementia and parkinsonism are associated with cotton wool plaques in the cortex and striatum. *Acta Neuropathol.* 104:155-170.
21. Takao M et al. (2001) Ectopic white matter neurons, a developmental abnormality that may be caused by the PSEN1 S169L mutation in a case of familial AD with myoclonus and seizures. *J. Neuropathol. Exp. Neurol.* 60:1137–52.
22. Marcon G et al. (2004) Neuropathological and clinical phenotype of an Italian Alzheimer family with M239V mutation of presenilin 2 gene. *J. Neuropathol. Exp. Neurol.* 63:199–209.
23. Mann DM, Pickering-Brown SM, Takeuchi A, and Iwatsubo T. (2001) Amyloid angiopathy and variability in amyloid beta deposition is determined by mutation position in presenilin-1-linked Alzheimer's disease. *Am. J. Pathol.* 158:2165–75.
24. Walker ES, Martinez M, Brunkan AL, and Goate A. (2005) Presenilin 2 familial Alzheimer's disease mutations result in partial loss of function and dramatic changes in Abeta 42/40 ratios. *J. Neurochem.* 92:294–301.
25. Bentahir M et al. (2006) Presenilin clinical mutations can affect gamma-secretase activity by different mechanisms. *J. Neurochem.* 96:732–42.
26. Parks AL and Curtis D. (2007) Presenilin diversifies its portfolio. *Trends Genet.* 23:140–50.
27. Handler M, Yang X, and Shen J. (2000) Presenilin-1 regulates neuronal differentiation during neurogenesis. *Development.* 127:2593–606.
28. Nishimura M et al. (1999) Presenilin mutations associated with Alzheimer disease cause defective intracellular trafficking of beta-catenin, a component of the presenilin protein complex. *Nat. Med.* 5:1–169.
29. Zhang Z et al. (1998) Destabilization of beta-catenin by mutations in presenilin-1 potentiates neuronal apoptosis. *Nature.* 395:698–702.
30. Berezovska O, Xia MQ, and Hyman BT. (1998) Notch is expressed in adult brain, is coexpressed with presenilin-1, and is altered in Alzheimer disease. *J. Neuropathol. Exp. Neurol.* 57:738–45.
31. Miele L and Osborne B. (1999) Arbiter of differentiation and death: Notch signaling meets apoptosis, *J. Cell Physiol.* 181:393–409.
32. Berezovska O, Jack C, Deng A, Gastineau N, Rebeck GW, and Hyman BT. (2001) Notch1 and amyloid precursor protein are competitive substrates for presenilin1-dependent gamma-secretase cleavage. *J. Biol. Chem.* 276:30018–23.
33. Lleo A, Berezovska O, Ramdya P, Fukumoto H, Raju S, Shah T, and Hyman BT. (2003) Notch1 competes with the amyloid precursor protein for gamma-secretase and down-regulates presenilin-1 gene expression. *J. Biol. Chem.* 278:47370–5.
34. Chang KA and Suh YH. (2005) Pathophysiological roles of amyloidogenic carboxy-terminal fragments of the beta-amyloid precursor protein in Alzheimer's disease. *J. Pharmacol. Sci.* 97:461–71.
35. Oster-Granite ML, McPhie DL, Greenan J, and Neve RL. (1996) Age-dependent neuronal and synaptic degeneration in mice transgenic for the C terminus of the amyloid precursor protein. *J. Neurosci.* 16:6732–41.
36. Song DK et al. (1998) Behavioral and neuropathologic changes induced by central injection of carboxyl-terminal fragment of beta-amyloid precursor protein in mice. *J. Neurochem.* 71:875–8.
37. Roher AE et al. (1993) Structural alterations in the peptide backbone of beta-amyloid core protein may account for its deposition and stability in Alzheimer's disease. *J. Biol. Chem.* 268:3072–83.
38. Roher AE, Lowenson JD, Clarke S, Woods AS, Cotter RJ, Gowing E, and Ball MJ. (1993) beta-Amyloid-(1-42) is a major component of cerebrovascular amyloid deposits: implications for the pathology of Alzheimer disease. *Proc. Natl. Acad. Sci. U. S. A.* 90:10836–40.
39. Kuo YM, Emmerling MR, Woods AS, Cotter RJ, and Roher AE. (1997) Isolation, chemical characterization, and quantitation of A beta 3-pyroglutamyl peptide from neuritic plaques and vascular amyloid deposits. *Biochem. Biophys. Res. Commun.* 237:188–91.
40. Guntert A, Dobeli H, and Bohrmann B. (2006) High sensitivity analysis of amyloid-beta peptide composition in amyloid deposits from human and PS2APP mouse brain. *Neuroscience.* 143:461–75.
41. Gowing E, Roher AE, Woods AS, Cotter RJ, Chaney M, Little SP, and Ball MJ. (1994) Chemical characterization of A beta 17-42 peptide, a component of diffuse amyloid deposits of Alzheimer disease. *J. Biol. Chem.* 269:10987–90.
42. Kuo YM et al. (1996) Water-soluble Abeta (N-40, N-42) oligomers in normal and Alzheimer disease brains, *J. Biol. Chem.* 271:4077–81.
43. Roher AE et al. (1996) Morphology and toxicity of Abeta-(1-42) dimer derived from neuritic and vascular amyloid deposits of Alzheimer's disease. *J. Biol. Chem.* 271:20631–5.
44. Kuo YM et al. (2001) Comparative analysis of amyloid-beta chemical structure and amyloid plaque morphology of transgenic mouse and Alzheimer's disease brains. *J. Biol. Chem.* 276:12991–8.
45. Kalback W et al. (2002) APP transgenic mice Tg2576 accumulate Abeta peptides that are distinct from the chemically modified and insoluble peptides deposited in Alzheimer's disease senile plaques. *Biochemistry.* 41:922–8.
46. Roher AE et al. (2004) The human amyloid-beta precursor protein770 mutation V717F generates peptides longer than amyloid-beta-(40-42) and flocculent amyloid aggregates. *J. Biol. Chem.* 279:5829–36.
47. Van Vickle GD et al. (2007) TgCRND8 amyloid precursor protein transgenic mice exhibit an altered gamma-secretase processing and an aggressive, additive amyloid pathology subject to immunotherapeutic modulation. *Biochemistry.* 46:10317–27.
48. Qi-Takahara Y et al. (2005) Longer forms of amyloid beta protein: implications for the mechanism of intramembrane cleavage by gamma-secretase. *J. Neurosci.* 25:436–45.
49. Kuo YM et al. (2000) Elevated abeta42 in skeletal muscle of Alzheimer disease patients suggests peripheral alterations of AbetaPP metabolism. *Am. J. Pathol.* 156:797–805.
50. Kaether C and Haass C. (2004) A lipid boundary separates APP and secretases and limits amyloid beta-peptide generation. *J. Cell Biol.* 167:809–12.
51. Cordy JM, Hooper NM, and Turner AJ. (2006) The involvement of lipid rafts in Alzheimer's disease. *Mol. Membr. Biol.* 23:111–22.
52. Vetrivel KS et al. (2004) Association of gamma-

secretase with lipid rafts in post-Golgi and endosome membranes. *J. Biol. Chem*. 279:44945–54.
53. Ehehalt R, Keller P, Haass C, Thiele C, and Simons K. (2003) Amyloidogenic processing of the Alzheimer beta-amyloid precursor protein depends on lipid rafts. *J. Cell Biol*. 160:113–23.
54. Kawarabayashi T et al. (2004) Dimeric amyloid beta protein rapidly accumulates in lipid rafts followed by apolipoprotein E and phosphorylated tau accumulation in the Tg2576 mouse model of Alzheimer's disease. *J. Neurosci*. 24:3801–9.
55. Lai MT et al. (2006) A presenilin-independent aspartyl protease prefers the gamma-42 site cleavage. *J. Neurochem*. 96:118–25.
56. Marchesi VT. (2005) An alternative interpretation of the amyloid Abeta hypothesis with regard to the pathogenesis of Alzheimer's disease. *Proc. Natl. Acad. Sci. U. S. A*. 102:9093–8.
57. Curran AR and Engelman DM. (2003) Sequence motifs, polar interactions and conformational changes in helical membrane proteins. *Curr. Opin. Struct. Biol*. 13:412–7.
58. Wood WG, Schroeder F, Igbavboa U, Avdulov NA, and Chochina SV. (2002) Brain membrane cholesterol domains, aging and amyloid beta-peptides. *Neurobiol. Aging*. 23:685–94.
59. Yehuda S, Rabinovitz S, and Mostofsky DI. (2005) Essential fatty acids and the brain: from infancy to aging. *Neurobiol. Aging*. 26 Suppl 1:98–102.
60. Yu WH et al. (2005) Macroautophagy—a novel Beta-amyloid peptide-generating pathway activated in Alzheimer's disease. *J. Cell Biol*. 171:87–98.
61. Bredesen DE. (2007) Key note lecture: toward a mechanistic taxonomy for cell death programs. *Stroke*. 38:652-660.
62. Tsujimoto Y and Shimizu S. (2005) Another way to die: autophagic programmed cell death. *Cell Death. Differ*. 12 Suppl 2:1528–34.
63. Iwata N, et al. (2001) Metabolic regulation of brain Abeta by neprilysin. *Science*. 292:1550–2.
64. Farris W et al. (2003) Insulin-degrading enzyme regulates the levels of insulin, amyloid beta-protein, and the beta-amyloid precursor protein intracellular domain in vivo. *Proc. Natl. Acad. Sci. U. S. A*. 100:4162–7.
65. Miller BC et al. (2003) Amyloid-beta peptide levels in brain are inversely correlated with insulysin activity levels in vivo. *Proc. Natl. Acad. Sci. U. S. A*. 100:6221–6.
66. Oefner C, D'Arcy A, Hennig M, Winkler FK, and Dale GE. (2000) Structure of human neutral endopeptidase (Neprilysin) complexed with phosphoramidon. *J. Mol. Biol*. 296:341–9.
67. Shen Y, Joachimiak A, Rosner MR, and Tang WJ. (2006) Structures of human insulin-degrading enzyme reveal a new substrate recognition mechanism. *Nature*. 443:870–4.
68. Morelli L et al. (2003) Differential degradation of amyloid beta genetic variants associated with hereditary dementia or stroke by insulin-degrading enzyme. *J. Biol. Chem*. 278:23221–6.
69. Morelli L et al. (2005) Insulin-degrading enzyme degrades amyloid peptides associated with British and Danish familial dementia. *Biochem. Biophys. Res. Commun*. 332:808–16.